

Cross-talk free selective reconstruction of individual objects from multiplexed optical field data



Alejandro Velez Zea^{a,*}, John Fredy Barrera^b, Roberto Torroba^{a,c}

^a Centro de Investigaciones Ópticas (CONICET La Plata-CIC-UNLP) C.P 1897, La Plata, Argentina

^b Grupo de Óptica y Fotónica, Instituto de Física, Facultad de Ciencias Exactas y Naturales, Universidad de Antioquia UdeA, Calle 70 No. 52-21, Medellín, Colombia

^c UIDET OPTIMO, Facultad de Ingeniería, Universidad Nacional de La Plata, La Plata, Argentina

ARTICLE INFO

Keywords:

Optical processing
Multiplexing
Compression
Holography

ABSTRACT

In this paper we present a data multiplexing method for simultaneous storage in a single package composed by several optical fields of tridimensional (3D) objects, and their individual cross-talk free retrieval. Optical field data are extracted from off axis Fourier holograms, and then sampled by multiplying them with random binary masks. The resulting sampled optical fields can be used to reconstruct the original objects. Sampling causes a loss of quality that can be controlled by the number of white pixels in the binary masks and by applying a padding procedure on the optical field data. This process can be performed using a different binary mask for each optical field, and then added to form a multiplexed package. With the adequate choice of sampling and padding, we can achieve a volume reduction in the multiplexed package over the addition of all individual optical fields. Moreover, the package can be multiplied by a binary mask to select a specific optical field, and after the reconstruction procedure, the corresponding 3D object is recovered without any cross-talk. We demonstrate the effectiveness of our proposal for data compression with a comparison with discrete cosine transform filtering. Experimental results confirm the validity of our proposal.

© 2017 Elsevier Ltd. All rights reserved.

1. Introduction

Since the seminal work by Gabor et al [1], holography remains a field with vast applications, including metrology [2] and microscopy [3]. In particular, the advances in computing together with low cost and high resolution digital cameras have made digital holography an important tool in optical processing techniques due to its great versatility and applicability. During last years, digital holography has been used in optical security [4–6], reconstruction of amplitude and phase [7], deformation measurement, synthesis and display of dynamic holographic 3D scenes [8], 3D measurements, dynamic digital holographic interferometry [9], phase-shifting color digital holography [10], improvements in spatial resolution [11], among others.

There is a variety of possible configurations for registering digital holograms, like on-line holography with phase shifting, off axis holography, self-interference holography, and coherent optical correlators, among others. The reasons for choosing a specific setup depend on the desired application and the available equipment. For example, off axis holography only requires a single shot to register the entire object information, but limits the bandwidth of the registered object, while on-line holography ensures maximum utilization of the sensor resolution at the

cost of requiring several holograms and additional elements in the experimental setup. Correlators, however, produce holograms containing the correlation between the object and any desired function. This capability is of importance in pattern recognition and optical security [6]. Some of the techniques developed for correlators can be applied to off-axis and on-line holographic setups [12].

On the other hand, processing of holographic information presents issues, like the noise in the reconstructed objects [13–15], and the fact that high quality digital hologram recording requires high resolution sensors, leading to large data volumes to be stored, transmitted and processed.

In this sense, compression of holographic data is a problem that needs to be addressed. Several methods have been proposed to achieve data compression of digital holograms, using a variety of approaches depending on the type of holographic data. Amongst these approaches we find the use of quantization [16], digital scaling of the holograms [17], and applications of digital algorithms for lossless and lossy compression [17–21]. Some of the most well know compression methods used for images and holograms perform a spectral filtering and quantization of the input data by means of Fourier, discrete cosine or wavelet transforms [21–24]. Some of these compression techniques show reduced performance when dealing with random or near random signals [25]. This makes them unsuitable for compression of the near random phase found in the optical fields produced by diffuse objects [26]. In this sense, opti-

* Corresponding author.

E-mail address: alejandrov@ciop.unlp.edu.ar (A.V. Zea).

cal compression may present higher or similar performance than digital methods for holographic data [27,28], with the added advantage of their potential deployment in actual optical systems.

One of the main techniques for handling multiple holographic data is multiplexing, which combines several holograms into a single package, in such a way that the resulting package could be later processed to extract the information of each individual hologram. To deal with these challenges, different approaches have been developed to achieve holographic data multiplexing using: multiple wavelengths [29], modulation with gratings [30,31] and spatial positioning [32]. These approaches are of interest in many cases, like: the use of multiple reference beams coming from the same source in pulsed digital holography [33], tilted wavefronts for superresolution [34], specially fabricated masks in order to obtain multiple digital image holograms [33], the shifting or rotating the real-world object [8] or any element of the experimental setup [35], several wavelengths in color digital holographic interferometry [9] and phase-shifting color digital holography [10], recorded images of an object under illumination from multiple angles [11], and multiples images registered with a moving detector [36].

However, we find that spatial and angular multiplexing are limited by: (a) the position of the objects in the reconstruction plane to ensure that there is no cross-talk between them, (b) the maximum possible frequency of the modulation gratings for a given hologram resolution, and (c) the fact that there is no way to retrieve the optical field data of a single object before reconstruction.

Davis & Cottrell [37] proposed multiplexing phase only filters using complementary random binary masks. The resulting hybrid filter behaves like a linear combination of both filter functions and the weight of each individual filter function could be controlled by the ratio of white pixels between the binary masks. Although the proposal was effective in demonstrating the method, it was limited to simple phase only filter functions. When dealing with digital holograms of diffuse 3D objects, we must take into account that the optical field data contains both amplitude and phase.

Also, one of the main limitations of the use of binary masks is that they induce a loss of information, however holographic data is inherently redundant [38]. This allows for reconstructing the object from partial or occluded optical fields. Furthermore, we can increase the redundancy of this data by performing a digital padding procedure of the optical field data, ensuring an increased resistance to the loss due to sampling at the cost of larger data volume [39]. Padding has been successfully employed for optical information processing in topics such as multiplexing of optically encrypted data [16,31,40–42] and optical field compression [27,28,43].

Our proposal combines this padding procedure and binary masks to achieve multiplexing without significant quality loss. We show that the binary mask can be conceived as a “selector key” that allows extracting only certain objects from the multiplexed package prior to reconstruction. In this way, the position of the objects to avoid superposition in the reconstruction plane is no longer necessary [44]. Additionally, depending on the padding used, and the number of objects to be multiplexed, the resulting package can have reduced volume, thus achieving multiplexing and compression simultaneously for the optical fields of diffuse objects.

2. Hologram recording, filtering and padding

In order to demonstrate our proposal, we require the phase and amplitude of the optical fields of several objects. There are several possible methods to obtain this data, however in this work we use an off-axis Fourier holography setup (Fig. 1) to record the holograms of three 3D objects [38]. A filtering procedure is then applied to the holograms in order to recover the phase and amplitude of the corresponding optical field [45], as shown next.

One of the arms provides a reference beam given by

$$R(v, w) = Ae^{2\pi if(v \sin \alpha + w \sin \beta)} \quad (1)$$

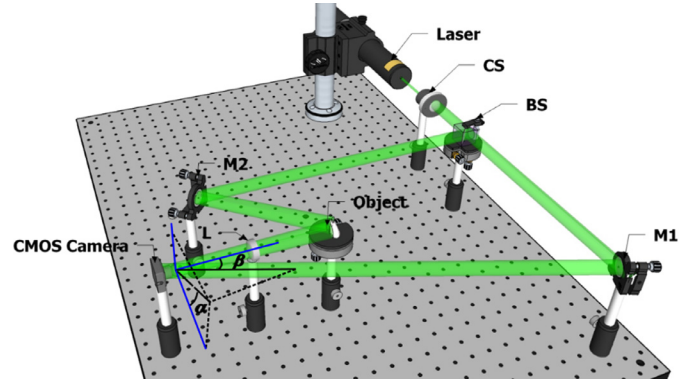


Fig. 1. Off-axis Fourier holographic setup (CS: collimation system, BS: beam splitter, M: mirror, L: lens, α , β : reference beam incidence angles).

where A is a constant beam amplitude, λ the wavelength, f the lens focal length and α and β the incidence angles and $v = x/\lambda f$ $w = y/\lambda f$ the coordinates in the CMOS camera plane.

This reference beam interferes in the CMOS plane with the Fourier transform (FT) of the light reflected by the 3D object, allowing the capture of the hologram, given as

$$H(v, w) = |A|^2 + |O(v, w)|^2 + O(v, w)e^{-2\pi if(v \sin \alpha + w \sin \beta)} + O^*(v, w)e^{2\pi if(v \sin \alpha + w \sin \beta)} \quad (2)$$

where $*$ means complex conjugate and $O(v, w)$ is the optical field data corresponding to the FT of the light reflected by the object $o(x, y)$.

Since the only data necessary to reconstruct the object is the optical field given by the function $O(v, w)$, we can filter this term and discard the remainder terms of Eq. (2). To do this, we first must consider that the hologram represented by Eq. (2) is sampled with a CMOS camera. This results in a digital hologram that is a matrix of discrete elements with dimensions equal to the camera resolution. Once we have the information in this matrix representation, we can perform the discrete Fourier transform (DFT) of the digital hologram. This results in a new matrix representation of the object plane, containing a central order (corresponding to the Fourier transform of the first two terms of Eq. (2), after sampling), the reconstructed $o(x, y)$ object and its twin image [38]. These orders are separated due to the interference fringes arising from the angles of incidence of the reference wave on the camera plane, given by α and β .

Given an object with an extension of $N \times N$ pixels in the object plane, we can digitally take only the matrix elements containing the reconstructed object and place them in a new matrix with size $N' \times N'$, where $N' > N$. After performing the inverse discrete Fourier transform (IDFT) of this new matrix, we obtain a padded optical field data containing only the information needed for reconstruction with increased data redundancy. The padding percentage can be calculated as $(N'/N - 1)$.

3. Resistance to random sampling of the optical field data

Using the optical field data extracted from a hologram with the procedure described above, we proceed to test the resistance to random sampling. To do this, we generated random binary masks of the same size as the optical fields. These masks have set percentage of pixels with value unity (a white pixel) and the remaining pixels have value zero. We multiply the optical field with binary masks with decreasing percentages of white pixels [37]. We measure the quality loss by calculating the normalized mean square error (NMSE) between the reconstruction from the optical field $I(p, q)$, and the reconstruction from the optical field multiplied by a binary mask with decreasing percentages of white pixels

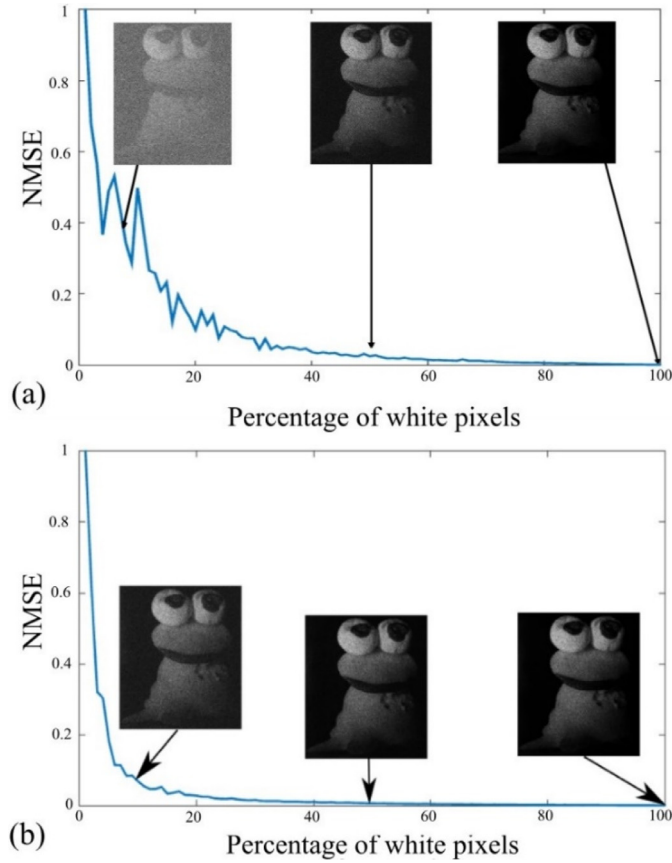


Fig. 2. NMSE curves between the reconstructed 3D objects from an optical field multiplied by binary masks of decreasing percentages of white pixels and without binary masks. Inset figures correspond to 100% white pixels (reference), 50% and 10%. (a) NMSE curve corresponding to the sampling of the optical field of the original size, and (b) to the sampling of an optical field after padding.

$I'(p, q)$. The NMSE is defined as

$$NMSE = \frac{\sum_{p,q}^{N,M} |I(p, q) - I'(p, q)|^2}{\sum_{p,q}^{N,M} |I(p, q) - I_W(p, q)|^2} \quad (3)$$

where (p, q) are pixel coordinates in the object plane, $N \times M$ the optical field size in pixels and $I_W(p, q)$ the intensity of the recovered 3D object from the optical field sampled with a binary mask of 1% white pixels.

As show in Fig. 2, the reconstructed objects from sampled optical fields are very resistant to the loss due to the sampling with the binary masks. This resistance will depend on the number of pixels of the optical field data hologram, and increases with the padding procedure. Fig. 2(a) shows the degradation of the reconstructed object from the optical field without padding (original size was 1200×1200). In this case, the degradation becomes evident when the number of sampled pixels is less than 20% of the total. In Fig. 2(b), we show the NMSE after padding to a size of 3000×3000 pixels. Now the degradation is not significant, even when less than 10% of the total pixels are sampled, therefore proving that padding ensures increased data redundancy and higher tolerance to random sampling.

4. Multiplexing with binary masks

Multiplexing not only is desirable to ensure a more compact information-carrying unit because all data is combined in a single one, but also because reduces the amount of information to be stored, transmitted and received. This is usually accomplished by simply adding each

optical field, obtaining

$$M(v, w) = \sum_j^N O_j(v, w) \quad (4)$$

This multiplexed package $M(v, w)$ is reconstructed by performing an IFT. This reconstruction will simultaneously recover all multiplexed 3D objects. Therefore, if the data is not prepared beforehand the recovery procedure will result in cross-talk. Additionally, it is not possible to select a particular object to be recovered.

In order to solve these issues, we now proceed to multiplex into a single package the optical fields extracted from several holograms using the procedure of Section 2. Prior to multiplexing, we multiply each optical field by a random binary mask. Each binary mask contains a number of white pixels randomly distributed in the optical field space. These masks are complementary and orthogonal, so that the addition of the binary masks used to multiplex the optical fields is a white matrix; and also guarantees that two masks do not sample the same pixel.

Thus, the optical field data to be multiplexed is sampled randomly by the product with a binary mask $B(v, w)$, and the resulting product is added to form the new multiplexed package.

$$M_b(v, w) = \sum_j^N O_j(v, w) B_j(v, w) \quad (5)$$

Since two masks do not sample the same pixel, we can select the information of the desired optical field from the package by multiplying by the corresponding mask $B_i(v, w)$, obtaining the sampled hologram $O_i(v, w) B_i(v, w)$. After applying an IFT to this sampled optical field we get

$$HB(x, y) = o_i(x, y) \otimes b_i(x, y) \quad (6)$$

This last equation represents the reconstructed 3D object $o_i(x, y)$ convolved with the FT of the random binary mask, which will have a random noise as background and a sharp peak with maximum intensity equal to the mean intensity of $B_i(v, w)$. This behavior can be explained by considering a binary mask as a sum of discrete points randomly distributed in the object plane. After a FT, this random distribution will result in another random pattern, with a DC term that will be proportional to the amount of points. Taking advantage of this behavior, we can simplify the treatment of the reconstruction by approximating $b_i(x, y)$ to a Dirac delta function plus a low intensity random noise. As the number of white pixels in the binary mask decreases, the random noise found on its FT increases in intensity, giving rise to the increase of the NMSE of the reconstructed object, as shown in the curves of Fig. 2. The use of random binary masks is advantageous due to the sharp peak of its FT [46]. The FT of binary masks with non-random distributions might have extended central orders, resulting in blurry reconstruction and loss of specific frequencies. For example, vertical or horizontal interlacing, as used in some correlation setups, produce replicated images whose spacing will depend on the interlacing frequency [47].

The number of optical fields that can be multiplexed in a single package depends on the percentage of white pixels of the binary mask and the acceptable error after reconstruction. In the examples of Fig. 2 we see that for the original optical field size, we can multiplex two optical fields with an error of 0.03, and ten with an error of 0.4 (Fig. 2(a)). After padding, we can multiplex the same ten fields with an error of 0.1 (Fig. 2(b)). In this way, multiplexing with binary masks can be also conceived as a lossy compression of data.

In Fig. 3 we show a flow chart describing the procedure for multiplexing three objects. First, the holograms are recorded, filtered, and if desired, padded following the procedure of Section 2. Afterwards, an orthogonal set of binary masks are generated, each with a percentage of white pixels equal to $N' \times N'/M$, where $N' \times N'$ is the pixel size of the optical fields, and M the number of fields to be multiplexed. Each optical field is then multiplied by one of the binary masks, and the resulting sampled fields are added to form the multiplexed package. To recover a

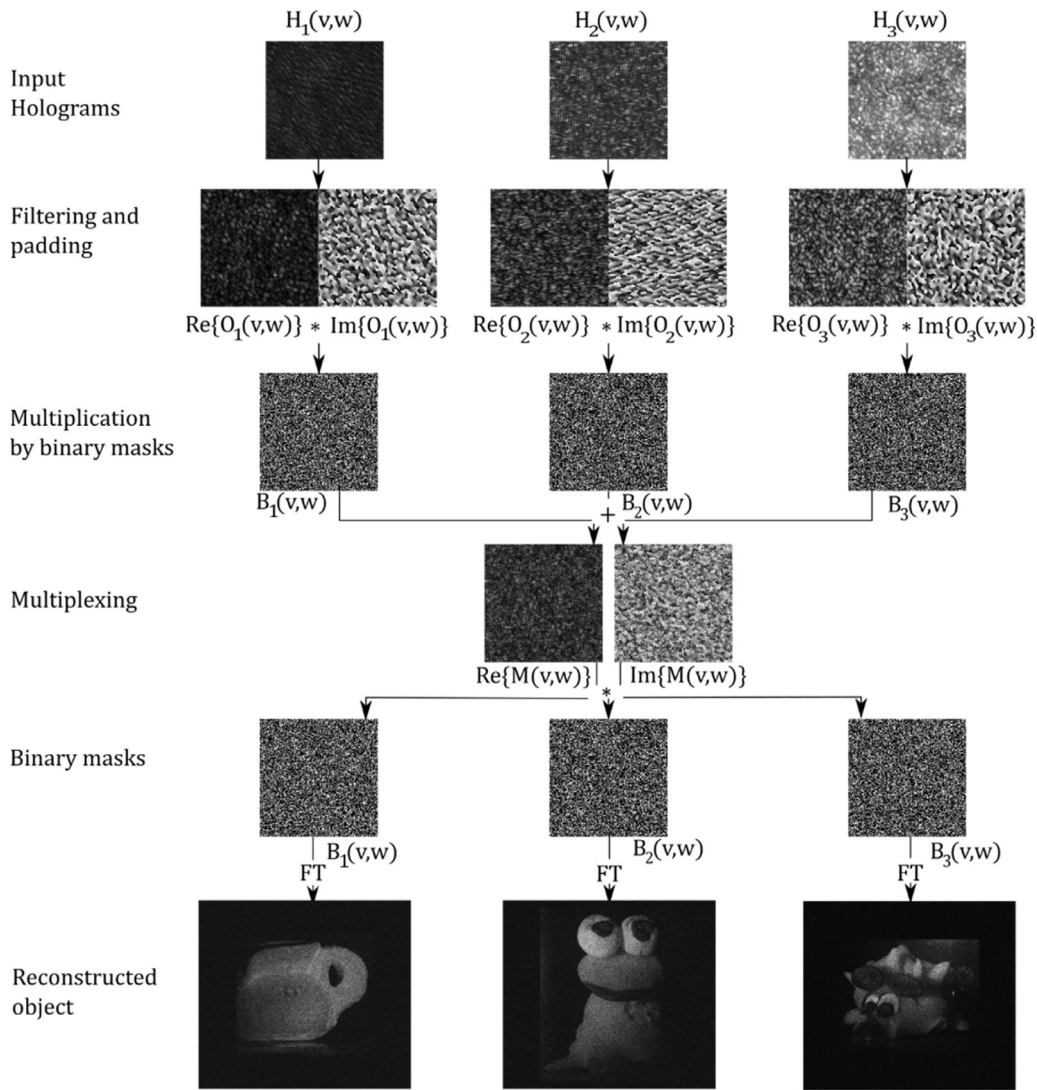


Fig. 3. Flow chart of the random binary mask multiplexing procedure. H: hologram, Re: Real part, Im: Imaginary part, O: optical field, B: binary mask, M: multiplexed package.

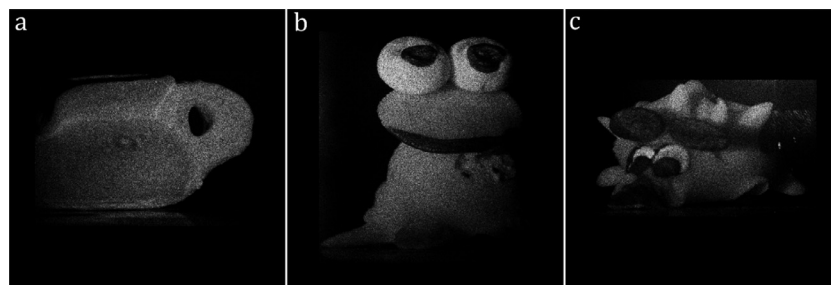


Fig. 4. Reconstructed objects from the optical fields used to test the multiplexing with random binary masks.

specific optical field, the multiplexed package is multiplied by the corresponding binary mask. Then, reconstruction can be accomplished by a FT.

In order to show the performance of the proposal, we used the scheme of Fig. 1 to register three holograms of 3D objects, using an EO-10,012M CMOS camera with a resolution of 3840×2748 pixels and $1.6 \mu\text{m}$ pixel size. In our setup, the incidence angles α and β of the reference wave were approximately 6° . We extracted the optical fields of each object with the filtering procedure detailed in Section 2, resulting in three 1200×1200 optical fields with zero padding. In Fig. 4 we show the reconstructed objects from these optical fields. The laser used

was a Laserglow Technologies DPSS laser with 532 nm wavelength and a power output of 50 mW. The 3D objects had maximum dimensions of $28 \times 15 \times 14 \text{ mm}^3$. The lens focal length was 200 mm.

In Fig. 5, we show the result of reconstruction three optical fields from a multiplexed package, with and without padding. For the first row, with no padding, the multiplexing package size was equal to the optical field size, at 1200×1200 pixels, and each field was sampled with binary masks with 33% white pixels. This means that the multiplexed package has a 66% volume reduction in comparison with the individual optical fields. The first column is the resulting objects when the package is reconstructed without any binary mask, and thus all ob-

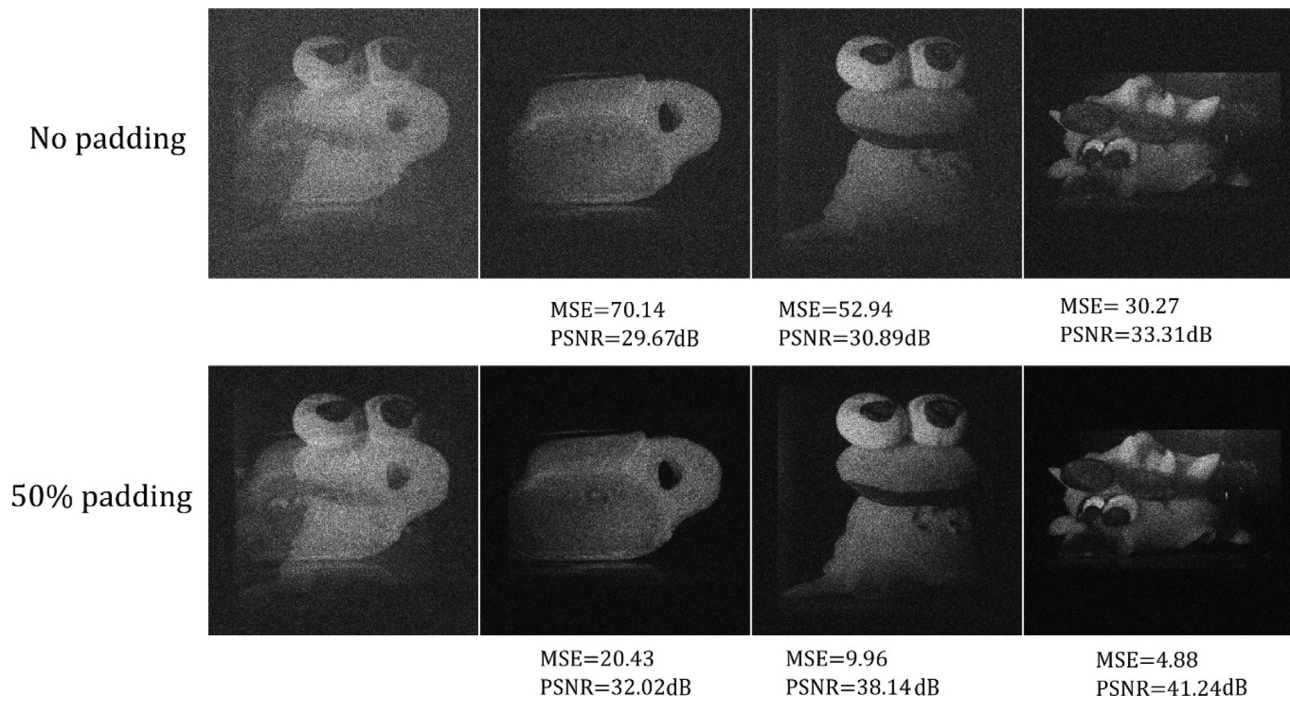


Fig 5. Reconstruction of optical fields from a multiplexed package of three different 3D objects with and without padding. First column is the reconstruction without any binary mask, and the remaining columns the reconstruction with the binary masks corresponding to each optical field.

jects appear overlapped, while in the remaining columns the package is reconstructed after multiplication with the binary masks corresponding to each of the original objects, without any traces of cross-talk. Notice the appearance of random noise when compared with the reconstructed objects without multiplexing shown in Fig. 5. In the second row, with the 50% padding, we show the same package when the multiplexed size is 1800×1800 pixels. This package has a 25% volume reduction over the individual optical fields, and the increased padding ensures reconstruction with less degradation due to the random sampling.

We want to quantify the degradation caused by the sampling with random binary masks. Therefore, we calculated both the mean square error (MSE) and the peak signal to noise ratio (PSNR) between the objects recovered without mask (Fig. 4) and those shown in Fig. 5. All used optical fields and their corresponding reconstructed objects are registered and stored with 8-bit depth. For data stored with this bit depth, values of the PSNR between 30 dB and 50 dB are typical in standard lossy compression techniques [48]. As seen in Fig. 5, all PSNR values fall within this range.

In Fig. 6 we show how the quality of the reconstructed object is affected by the application of sampling and padding simultaneously. This is achieved by taking the optical field corresponding to the object in Fig. 4(b), applying increasing percentages of padding and sampling with binary masks with decreasing percentages of white pixels. After reconstruction, we calculate the PSNR compared with the object reconstructed from the original optical field. As we can see from the plot, higher padding allows for sampling with less white pixels for the same PSNR. This means that increased padding allows for multiplexing more objects while maintaining acceptable reconstruction quality.

In order to further validate the effectiveness of random sampling for compression, we now compare with another technique for image compression based in the discrete cosine transform (DCT) [21]. In this scheme, each optical field is transformed with a DCT. The resulting transform is then filtered with a square whose area will determine the compression ratio and quality loss of the optical field. An inverse discrete cosine transforms (IDCT) is applied to decompress the field. After decompression, we perform the standard reconstruction method.

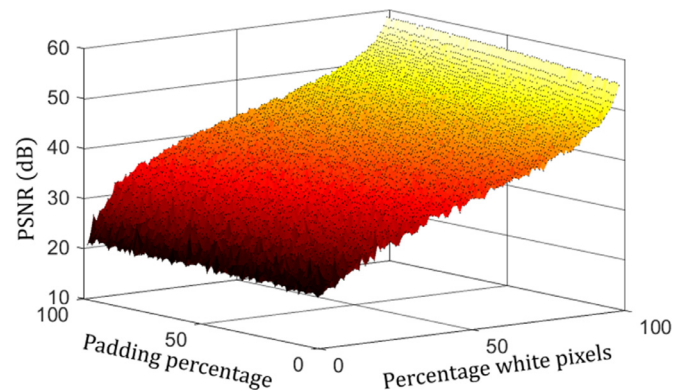


Fig. 6. PSNR between an object reconstructed from its original optical field and the same object reconstructed from an optical field with different amounts of padding and sampling with binary masks.

In Fig. 7 we show the results of DCT filtering lossy compression. As in the results show in Fig. 5, the first row is the results from optical fields of size 1200×1200 pixels, and the DCT filter size was 692×629 pixels, for volume reduction of 66%. In the second row, the optical fields were padded to a size of 1800×1800 . The DCT filter area was 1040×1040 , for a volume reduction of 25% over the original optical fields. As in the random sampling, padding decreases the loss due to DCT compression, at the cost of increased volume. Random sampling with binary masks maintains a higher MSE and PSNR for all objects with and without padding, demonstrating the validity of our proposal.

DCT filtering together with quantization of the resulting transform has been successfully applied to image data [21], however, it shows reduced performance when processing optical field data of near random objects. This highlights the need of alternative methods for holographic compression, especially when dealing with the quasi-random phases and amplitudes produced by diffuse objects. The results in this paper show that random binary mask sampling is one of those approaches, with the additional advantage of allowing selective reconstruction of individual objects

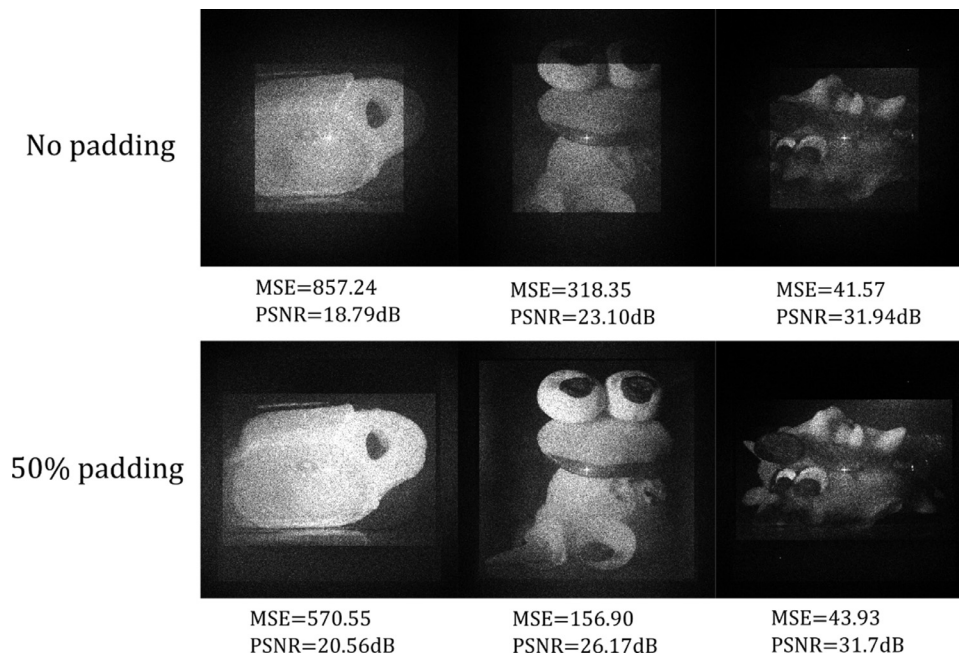


Fig. 7. Reconstructed objects from optical fields without padding and with 50% padding compressed with DCT filtering.

5. Conclusions

We consider the proposed technique useful to multiplex data with cross-talk free recovery, especially in two cases: (a) when minor data loss can be tolerated in exchange for the ability to select 3D objects from the multiplexed packages prior to reconstruction, and (b) when spatial or angular multiplexing is not feasible due to the size of the objects or the sample rates involved in the digital holograms. In our proposal, the bandwidth is affected neither by padding nor by multiplexing. This capability may be of use in optical security and displays, where a single package can contain different scenes to be recovered without cross talk only when processed with the adequate binary mask, thus making the binary mask a security key for optimal retrieval of the desired data, or by hiding watermarks or validation information. This can be achieved by sampling an optical field with a binary mask with a very large percentage of white pixels and multiplexing it with specially tailored watermark or validation data occupying the remaining pixels. In this way, the object sampled with more pixels will have higher intensity and appear nearly unaltered, while the watermark will only be revealed by multiplying the package with the adequate binary mask.

The random binary masks sample the optical field, causing frequency loss that results in decreasing the quality after reconstruction. However, the pixel size and the resolution of the optical field remain the same, and therefore the spatial bandwidth is not altered. Multiplexing causes no further changes in the information contained in the package, since all optical field are sampled with binary masks that are orthogonal between them. Padding increases the redundancy of the frequency information, and also the resistance of the optical fields to sampling. Padding is performed on the object plane, and it does not alter the spatial bandwidth.

Additionally, depending on the padding used and the acceptable object degradation, the multiplexed package can have a smaller data volume than the original optical fields. According to our findings, we can multiplex for instance ten optical fields with an NMSE error of 0.4 without padding, while the same error reduces to 0.1 when padding is applied. Our results show that an adequate selection of sampling with binary masks and padding leads to an alternative lossy data compression procedure, which offers increased performance when compared with DCT filtering compression. Furthermore, this multiplexing strategy can be implemented experimentally without inserting specially fabricated

masks, several wavelengths, multiple reference beams coming from the same source, shifting or rotating the real-world object or any element. Additionally, the objects are recovered using the same setup without inserting or moving any element, and all objects can be reconstructed in the same position, avoiding the displacement of the camera during recovery. Therefore, the recording and the recovering setups reduce some practical requirement as stability, and the number and complexity of the involved elements.

Acknowledgments

This research was performed under grants from Estrategia de Sostenibilidad 2014–2015 and Comité para el Desarrollo de la Investigación -CODI- (Universidad de Antioquia-Colombia), MINCYT-COLCIENCIAS CO/13/05, CONICET Nos. 0849/16 and 0549/12 (Argentina), and Facultad de Ingeniería, Universidad Nacional de La Plata No. 11/I215 (Argentina). John Fredy Barrera Ramírez acknowledges the support from the International Centre for Theoretical Physics ICTP Associate-ship Scheme.

References

- [1] Gabor D. A new microscopic principle. *Nature* 1948;161:777.
- [2] Baumbach T, Osten W, Kopylow C, Jüptner W. Remote metrology by comparative digital holography. *Appl Opt* 2006;45:925.
- [3] Zhang T, Yamaguchi I. Three-dimensional microscopy with phase-shifting digital holography. *Opt Lett* 1998;23:1221.
- [4] Velez A, Barrera JF, Torroba R. Three-dimensional joint transform correlator cryptosystem. *Opt Lett* 2016;41:599.
- [5] Barrera JF, Mira A, Torroba R. Optical encryption and QR codes: secure and noise-free information retrieval. *Opt Express* 2013;21:5373.
- [6] Javidi B, Carnicer A, Yamaguchi M, Nomura T, Pérez-Cabré E, Millán MS, et al. Roadmap on optical security. *J Opt* 2016;18:083001.
- [7] Paturzo M, Memmolo P, Miccio L, Finizio A, Ferraro P, Tulino A, et al. Numerical multiplexing and demultiplexing of digital holographic information for remote reconstruction in amplitude and phase. *Opt Lett* 2008;33:2629.
- [8] Paturzo M, Memmolo P, Finizio A, Näsänen R, Naughton TJ, Ferraro P. Synthesis and display of dynamic holographic 3D scenes with real-world objects. *Opt Express* 2010;18:8806.
- [9] Demoli N, Vukicevic D, Torzynski M. Dynamic digital holographic interferometry with three wavelengths. *Opt Express* 2003;11:767.
- [10] Yamaguchi I, Matsumura T, Kato J. Phase-shifting color digital holography. *Opt Lett* 2002;27:1108.
- [11] Thurman ST, Bratcher A. Multiplexed synthetic-aperture digital holography. *Appl Opt* 2015;54:559.

- [12] Zalevsky Z, Rubner A, Garcia J, Garcia-Martinez P, Ferreira C, Marom E. Joint transform correlator with spatial code division multiplexing. *Appl Opt* 2006;45:7325–33.
- [13] Vilardy JM, Millán MS, Perez-Cabr e E. Improved decryption quality and security of a joint transform correlator-based encryption system. *J Opt* 2013;15:025401.
- [14] Barrera JF, Velez A, Torroba R. Experimental scrambling and noise reduction applied to the optical encryption of QR codes. *Opt Express* 2014;22:20268.
- [15] Bianco V, Memmolo P, Paturzo M, Finizio A, Javidi B, Ferraro P. Quasi noise-free digital holography. *Light Sci Appl* 2016;5:e16142.
- [16] Mills GA, Yamaguchi I. Effects of quantization in phase-shifting digital holography. *Appl Opt* 2005;44:1216–25.
- [17] Naughton TJ, Frauel Y, Javidi B, Tajahuerce E. Compression of digital holograms for three-dimensional object reconstruction and recognition. *Appl Opt* 2002;41:4124–32.
- [18] Alfalou A, Brosseau C. Optical image compression and encryption methods. *Adv Opt Photon* 2009;1:589–636.
- [19] Alfalou A, Brosseau C. Implementing compression and encryption of phase-shifting digital holograms for three-dimensional object reconstruction. *Opt Commun* 2013;307:67–72.
- [20] Huffman DA. A method for the construction of minimum-redundancy codes. In: *Proceedings of the I.R.E.*; 1952. p. 1098–101.
- [21] Alfalou A, Brosseau C, Abdallah N, Jridi M. Simultaneous fusion, compression, and encryption of multiple images. *Opt Express* 2011;19:24023–9.
- [22] Alfalou A, Brosseau C, Abdallah N, Jridi M. Assessing the performance of a method of simultaneous compression and encryption of multiple images and its resistance against various attacks. *Opt Express* 2013;21:8025–43.
- [23] Wallace GK. The JPEG still picture compression standard. *IEEE Trans Consum Electron* 1992;38 xviii–xxxiv.
- [24] Bang LT, Ali Z, Quang PD, Park JH, Kim N. Compression of digital hologram for three-dimensional object using Wavelet–Bandelets transform. *Opt Express* 2011;19:8019–31.
- [25] Shahnaz R, Walkup JF, Krile TF. Image compression in signal-dependent noise. *Appl Opt* 1999;38:5560–7.
- [26] Darakis E, Soraghan JJ. Compression of interference patterns with application to phase-shifting digital holography. *Appl Opt* 2006;45:2437–43.
- [27] Trejos S, Barrera JF, Velez A, Tebaldi M, Torroba R. Optical approach for the efficient data volume handling in experimentally encrypted data. *J Opt* 2016;18:065702.
- [28] Velez A, Barrera JF, Trejos S, Tebaldi M, Torroba R. Optical field data compression by optodigital means. *J Opt* 2016;18:125701.
- [29] Tahara T, Mori R, Kikunaga S, Arai Y, Takaki Y. Dual-wavelength phase-shifting digital holography selectively extracting wavelength information from wavelength-multiplexed holograms. *Opt Lett* 2015;40:2810.
- [30] Paturzo M, Memmolo P, Tulino A, Finizio A, Ferraro P. Investigation of angular multiplexing and de-multiplexing of digital holograms recorded in microscope configuration. *Opt Express* 2009;17:8709.
- [31] Trejos S, Barrera JF, Tebaldi M, Torroba R. Experimental opto-digital processing of multiple data via modulation, packaging and encryption. *J Opt* 2014;16:055402.
- [32] Sha B, Liu X, Ge X, Guo C. Fast reconstruction of off-axis digital holograms based on digital spatial multiplexing. *Opt Express* 2014;22:23066.
- [33] Yuan C, Zhai H, Liu H. Angular multiplexing in pulsed digital holography for aperture synthesis. *Opt Lett* 2008;33:2356.
- [34] Mico V, Zalevsky Z, Garc a-Mart nez P, Garc a J. Superresolved imaging in digital holography by superposition of tilted wavefronts. *Appl Opt* 2006;45:822.
- [35] Mico V, Zalevsky Z, Garc a-Mart nez P, Garc a J. Synthetic aperture superresolution with multiple off-axis holograms. *J Opt Soc America A* 2006;23:3162.
- [36] Le Clerc F, Gross M, Collot L. Synthetic-aperture experiment in the visible with on-axis digital heterodyne holography. *Opt Lett* 2001;26:1550.
- [37] Davis JA, Cottrell DM. Random mask encoding of multiplexed phase-only and binary phase-only filters. *Opt Lett* 1994;19:496.
- [38] Schnars U, Jueptner W. *Digital holography: digital hologram recording, numerical reconstruction, and related techniques*. 1st ed. Berlin: Springer Verlag GmbH; 2005.
- [39] Ferraro P, Nicola S, Coppola G, Finizio A, Alfieri D, Pierattini G. Controlling image size as a function of distance and wavelength in Fresnel-transform reconstruction of digital holograms. *Opt Lett* 2004;29:854.
- [40] Barrera JF, Velez A, Torroba R. Experimental multiplexing protocol to encrypt messages of any length. *J Opt* 2013;15:055404.
- [41] Chen W, Chen X. Optical multiple-image encryption based on multiplane phase retrieval and interference. *J Opt* 2011;13:115401.
- [42] Saini N, Sinha A. Video encryption using chaotic masks in joint transform correlator. *J Opt* 2015;17:035701.
- [43] Alfalou A, Elbouz M, Mansour A, Keryer G. New spectral image compression method based on an optimal phase coding and the RMS duration principle. *J Opt* 2010;12:115403.
- [44] Velez A, Barrera JF, Torroba R. One-step reconstruction of assembled 3D holographic scenes. *Opt Laser Tech* 2015;75:146.
- [45] Cuhe E, Marquet P, Depeursing C. Spatial filtering for zero-order and twin-image elimination in digital off-axis holography. *Appl Opt* 2000;39:4070–5.
- [46] Goodman JW. *Introduction to Fourier optics*. 2nd ed. New York: McGraw-Hill; 1996.
- [47] Zalevsky Z, Garc a J, Garc a-Mart nez P. Interlacing multiplexing techniques for optical morphological correlation. *Opt Commun* 2006;264:45–50.
- [48] Welstead ST. *Fractal and wavelet image compression techniques*. Washington: SPIE Optical Engineering Press; 1999.



Alejandro Velez Zea received his BSc degree in physics from Antioquia University (Medellin, Colombia) in 2014. He is now a PhD student at the Center for Optical Research of La Plata (CIOP), Argentina and teacher assistant in the School of Engineering at the University of La Plata in Argentina. He has published 10 peer reviewed papers in international journals, with research centered around optical encryption, digital holography and optical data compression.



John Fredy Barrera Ramírez received his BSc, MSc, and PhD degrees in physics from Antioquia University (Medellín, Colombia) in 2001, 2003, and 2007, respectively. Since 2006 he has been with Antioquia University, where he is Professor in the Physics Institute and coordinator of the Optics and Photonic's Group. He is “Junior Associate” of the International Centre for Theoretical Physics and “Young Affiliate” of the World Academy of Sciences, “Senior Member” of the Optical Society and member of the International Society for Optics and Photonics. He has authored 48 peer-reviewed international papers, one invention patent, 18 publications in international conference proceedings and 18 publications in national peer-reviewed journals with more than 960 citations.



Professor Roberto Torroba, published over 120 papers in peer reviewed journals, and a number of contributions in Congresses around the world. He serves as reviewer in international journals, supervised several doctoral thesis, and much of his work was highlighted and distinguished in prestigious journals. Presently he is Member of the Argentinean research council as Superior Researcher, full Professor at the School of Engineering at the University of La Plata in Argentina and Director of the Unit of Research and Development “OPTIMO”. His areas of interest are in the field of optical processing, encryption and validation, digital holography and virtual optics.